CO4-1 Influence of γ-Ray Irradiation Conditions on Encapsulation of Hydrogen Atom into Silsesquioxane

Y. Okaue, T. Yokoyama and T. Sakudo

Department of Chemistry, Faculty of Sciences, Kyushu University

INTRODUCTION: Trimethylsilylated silsesquioxane, Q_8M_8 ($[(CH_3)_3SiO]_8(SiO_{1.5})_8$), is a member of the cage-shaped oligosilsesquioxanes with cubic framework called double four-ring (D4R) structure as illustrated in Fig. 1. Upon ^{60}Co γ-ray irradiation at room temperature on Q_8M_8, a stable hydrogen atom is encapsulated in the D4R cage. The encapsulation and stabilization of a hydrogen atom in the D4R cage were confirmed by ESR spectroscopy.[1] However, the amount of the hydrogen atom encapsulated in the D4R cage of Q_8M_8 was a little. Under 100 kGy irradiation, the amount was about 1/20,000 per Q_8M_8 molecule. The purpose of this study was to estimate the amounts of the hydrogen atom encapsulated in the D4R cage of Q_8M_8 under various γ-ray irradiation conditions by ESR. In addition, to encapsulate hydrogen atom in the D4R cage of Q_8M_8 more efficiently, the coexistence materials such as hexane were added for the source of hydrogen atom before γ-ray irradiation, and the amounts of the hydrogen atom in the D4R cage of the irradiated Q_8M_8 were also estimated by ESR.

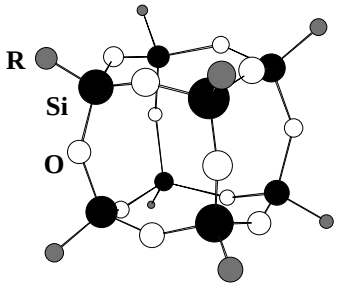

Fig. 1. D4R cage structure of silsesquioxane.
R = $(CH_3)_3SiO$; Q_8M_8

EXPERIMENTS: Q_8M_8 used in this study was prepared by trimethylsilylation of octameric tetramethylammonium silicate ($[(CH_3)_4N]_8(SiO_{1.5})_8$). ^{60}Co γ-ray irradiation experiments to Q_8M_8 (1 g) were carried out at total dose of 340-1700 kGy under air at room temperature. ESR spectra were measured at room temperature with the same amount of the irradiated Q_8M_8 after recrystallization from hexane. If necessary, coexistence materials were added before the γ-ray irradiation and removed by recrystallization before ESR measurements.

RESULTS: As shown in Fig. 2, ESR spectrum of the irradiated Q_8M_8 at room temperature showed characteristic two hyperfine lines separated with 50.8 mT due to hydrogen atom encapsulated in the D4R cage. The average of the height of the two lines was considered to be signal intensity. From the signal intensity, the amount of the encapsulated hydrogen atom in the D4R cage of the irradiated Q_8M_8 was evaluated.

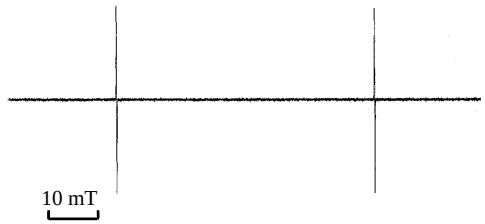

Fig. 2. ESR spectrum of the hydrogen atom encapsulated in the D4R cage of Q_8M_8 after γ-ray irradiation.

The correlation of the ESR signal intensity for the encapsulated hydrogen atom in the D4R cage of the irradiated Q_8M_8 and the irradiation dose of γ-ray was shown in Fig. 3. ESR signal intensity increases with increasing the irradiation dose. It was shown that the amount of the encapsulated hydrogen atom in the D4R cage of the irradiated Q_8M_8 increases with increasing the irradiation dose.

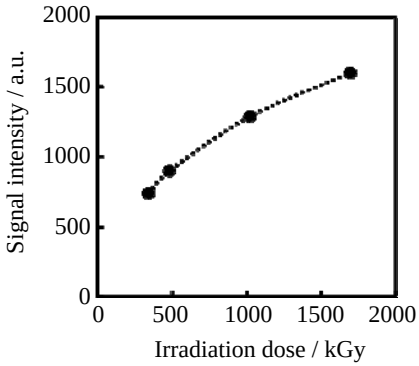

Fig. 3. Correlation of the ESR signal intensity for the encapsulated hydrogen atom in the D4R cage of Q_8M_8 and the irradiation dose of γ-ray.

Some alkanes and cycloalkanes were used as the coexistence materials for the source of hydrogen atom but systematic results were not obtained.

REFERENCE:

[1] R. Sasamori, Y. Okaue, T. Isobe, Y. Matsuda, Science, **265** (1994) 1691-1694.

採択課題番号 21008　　ガンマ線照射条件がシルセスキオキサンの水素原子捕捉に及ぼす影響　　共同通常

（九大院理）岡上吉広、横山拓史、作道　翔

CO4-2 Coherent Excitation of Superionic Conduction

T. Awano and T. Takahashi[1]

Department of Electronic Engineering, Tohoku Gakuin University
[1]Research Reactor Institute, Kyoto University

INTRODUCTION: Movement of ions is not in phase and frequent scattering by other mobile ions seems to decrease the ionic conductivity. If coherent excitation of ionic movement by coherent external electric field occurs, ionic conductivity seems to increase drastically. We have investigated sub-millimeter and far-infrared spectroscopy of superionic conductors to find such a correlative movement of conduction ion. Ionic plasmon absorption was observed at sub-millimeter region of MA_4X_5 (M=Rb, K, NH_4; A=Ag or Cu; X=I or Cl) crystals [1]. Coherent THz wave from LINAC of KURRI is so strong that the excitation effect is expected to be observed. We have measured millimeter wave absorption spectra of silver halides - silver phosphate glasses to investigate the existence of such a collective movement of conduction ion [2]. In this study, copper ion conductors were investigated to compare spectral deference by the mass of conduction ion.

EXPERIMENTS: Each content of CuI, Cu_2O and P_2O_5 were melt in Pyrex tube with N_2 atmosphere at 600 C for 30 min. Then the melt was quenched in water. Sample pellets with thicknesses around 1mm were obtained by pressing. Transmittance spectra of coherent millimeter wave were measured by a Martin-Puplett type interferometer.

RESULTS: Figure 1 shows absorption spectra of a CuI-$CuPO_3$ glass. Increment spectra from absorption at 77K are shown to avoid interference fringe structure. Two absorption bands were observed as those in AgI-$AgPO_3$ glasses. Peak positions are, however, slightly different. They are 9.9 and 6.8 cm^{-1} for each temperature in the CuI-$CuPO_3$ glass, while they are 8.5 and 6.1 cm^{-1} AgI-$AgPO_3$ glasses. The peak positions of these bands are 15% and 10% larger than those in the AgI-$AgPO_3$ glasses. This seems to be due to difference of conduction ions, copper and silver. However, this ratio is smaller than that of the square root of the mass of conduction ion (1.3). This suggests that these bands are due to not only one mobile ion but also other ions. This is consistent with the result in bromides-silver phosphate glasses [3].
Figure 2 shows absorption spectra of $(TMAI)_{0.15}(TEAI)_{0.1}(CuI)_{0.75}$ glass. Main feature of the spectra is the same as that of CuI-$CuPO_3$ glass. There were additional absorption in low and high energy side of the bands. The origin of these absorption is not clear yet.

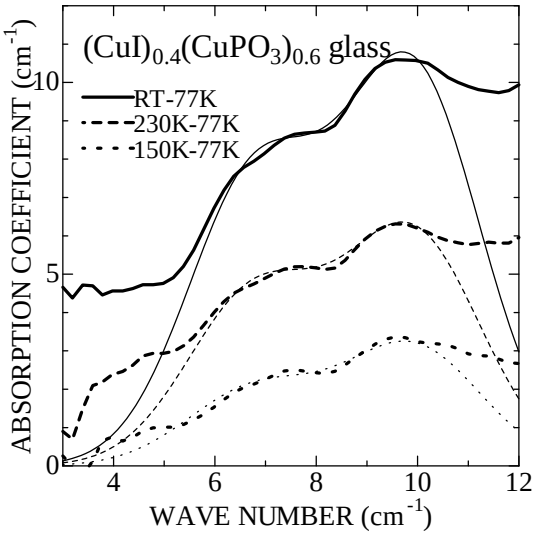

Fig.1. Increment absorption spectra of $(CuI)_{0.4}(CuPO_3)_{0.6}$ glass from that at 77K. Thin lines show the summation of two Gaussian curves at 9.9 and 6.8 cm^{-1} for each temperature.

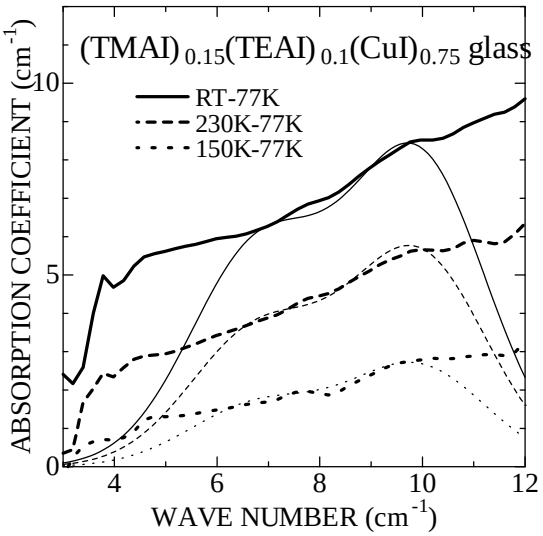

Fig.2. Increment absorption spectra of $(TMAI)_{0.15}(TEAI)_{0.1}(CuI)_{0.75}$ glass from that at 77K. Thin lines show the summation of two Gaussian curves with the same parameters as those in Fig. 1.

REFERENCES:

[1] T. Awano, Infrared Physics and Technology **51**(2008) 458.

[2] T. Awano and T. Takahashi, Journal of Physics: Conference Series **148** (2009) 012040.

[3] T. Awano and T. Takahashi,J. Phys. Soc. Jpn. **79** Suppl. A (2010) 118.

採択課題番号 21011　　超イオン導電体におけるコヒーレントミリ波誘起イオン伝導の検証　　共同通常

（東北学院大・工）淡野照義　（京大・原子炉）高橋俊晴

CO4-3

Dependence of Gamma-ray Dose on Annihilation Behavior of Irradiation Defects in Li_2TiO_3

K. Okuno[1], Y. Oya[1], S. Suzuki[1], R. Kurata[1],
M. Kobayashi[1], H. Yamana[2], T. Fujii[2] and Y. Nakano[2]

[1]*Radioscience Research Laboratory, Faculty of Science, Shizuoka University*
[2]*Research Reactor Institute, Kyoto University*

INTRODUCTION: Several studies have been carried out to establish a tritium recovery system in fusion reactors. Especially, lithium titanate (Li_2TiO_3) is focused on since it is one of the candidates as the tritium breeding material of ITER. In our previous studies, it has been reported for the neutron-irradiated Li_2TiO_3 that there was a correlation between the tritium release and the annihilation of irradiation defects, especially E'-center which was oxygen vacancy occupied by one electron. For this reason, the behavior of irradiation defects is an important issue to understand the tritium behavior in Li_2TiO_3. However, it has not been clarified in detail the correlation between the formation and annihilation processes of the irradiation defects because they were produced by not only collision process but also electron-excitation process during neutron irradiation [1].The electron-excitation process occurres by gamma-ray irradiation. Therefore, in this study gamma-ray irradiation was adopted to produce irradiation defects only by the electron-excitation process.

In this study, the electron spin resonance (ESR) method was used to detect the irradiation defects such as E'-center which has unpaired electron in Li_2TiO_3 irradiated by gamma-ray with various gamma-ray dose. The isochronal annealing experiments were performed to understand the annihilation behavior of the irradiation defects.

EXPERIMENTS: The Li_2TiO_3 powder purchased from Furuuchi chemistry Co. Ltd. was irradiated by gamma-ray (dose rate: 2.5 kGy h^{-1}, temperature: room temperature) with the dose of 45-240 kGy at the Co-60 Gamma-ray Irradiation Facility in the Research Reactor Institute, Kyoto University. After irradiation, the irradiation defects in gamma-ray irradiated Li_2TiO_3 was measured by means of ESR at 77 K. Isochronal annealing experiments were performed in the temperature range of 298-798 K to determine annihilation temperature of irradiation defects. Isothermal annealing experiments were also performed at 423-673 K through a maximum heating time of 8 hours to understand annihilation kinetics of irradiation defects.

RESULTS: The ESR spectrum for gamma-ray irradiated Li_2TiO_3 consisted of two major peaks, one was E'-centers, and the other was O-related defects, which were oxygen hole centers such as O^--center and O_2^--center [2, 3]. These defects are known to be a Frenkel pair and disappeared by recombination each other [4]. Comparing the intensity of E'-center with that of O-related defects in various gamma-ray dose, it was found that these defects increased as increasing irradiation dose.

Figure shows the annihilation behavior of the irradiation defects in isochronal annealing experiments for 45 kGy gamma-ray irradiated sample and that for 75 kGy gamma-ray irradiated one.

From the results of isochronal experiments, it was found that the intensities of E'-center and O-related defects decreased at temperature region of 550-650 K for 45 kGy gamma-ray irradiated sample. On the other hand, those for gamma-ray irradiated one with the dose of more than 75 kGy were decreased at 300-400 K and 600-700 K. It was apparent that there is one annihilation stage for the former while there are two stages for the later. From the results of isothermal experiments, the activation energies of irradiation defects for the former and the later were 0.68±0.01 eV and 1.20±0.03 eV, respectively.

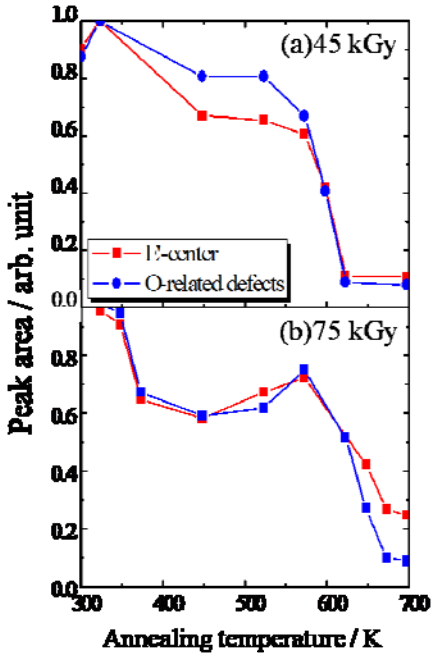

Fig. 1. Annihilation behaviors of the irradiation defects in isochronal annealing for 45 kGy and 75 kGy gamma-ray irradiated samples.

REFERENCES:

[1] M. Oyaidzu *et al., J. Nucl. Mater.*, **329-333** (2004) 1313-1317.
[2] Y. Bensimon *et al., J. Phys. Chem. Sol.*, **2000**, *61*, 1623-1632.
[3] Moritani *et al., J. Nucl. Mater.*. **2004**, *239-333*, 988-992.
[4] T. Oda, *et al., J. Nucl. Mater.*, **386-388** (2009) 1087-1090

採択課題番号 21013　　核融合炉トリチウム増殖候補材中トリチウムの移行過程に及ぼす照射効果　　共同通常

（静岡大・理・放射研）奥野 健二、大矢 恭久、鈴木 祥子、倉田 理江、小林 真
（京大炉）山名 元、藤井 俊行、上原 章寛、中野 幸廣

CO4-4 Absorption Spectroscopy with the Coherent THz Radiation from Linac Electron Beams

S. Okuda, T. Kojima, R. Taniguchi, D. Komatsu and T. Takahashi[1]

Radiation Research Center, Osaka Prefecture University
[1]Research Reactor Institute, Kyoto University

INTRODUCTION: Coherent synchrotron and transition radiation from electron bunches of a linear accelerator (linac) has a continuous spectrum at relatively high peak-intensity in a THz frequency range. Coherent radiation light sources for applications were first established in Kyoto University and Osaka University [1, 2].

Recently, the absorption spectroscopy system using the coherent transition radiation from the electron beams of the L-band electron linac has been established at KURRI [3]. With this system absorption spectroscopy has been carried out for various kinds of samples in our project [4].

In this article the results for the fine SiO_2 particles are reported. The electromagnetic wave in microwave and THz regions is applied to sintering processes of powder materials as a source for heating. However, the energy absorption process for heating is not well understood. In the present work absorption spectroscopy has been carried out for fine SiO_2 particles and the effect of the light intensity has also been investigated.

EXPERIMENTAL METHOD: The electron beams of the 46 MeV KURRI L-band linac were used for experiments. The configurations for the absorption spectroscopy are schematically shown in Fig. 1. Coherent transition radiation was emitted from an aluminum foil. Output light from a Martin-Puplett type interferometer, linearly polarized, was focused at a light collimator with 8 mmϕ diameter located just before a sample. The light path was in the air atmosphere. The detector was a liquid-He-cooled silicon bolometer.

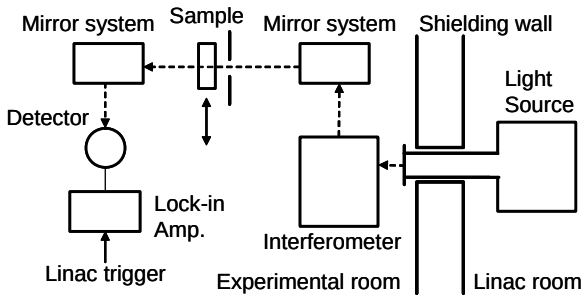

Fig. 1. Schematic diagram of the configurations for the absorption spectroscopy.

The wavenumber resolution was 0.2 cm^{-1} in the present experiments. It took about 5 minutes in a measurement. The light spectrum was obtained by averaging over four measurements. The spectrum was sufficiently stable during the measurements within ±2-3% in a wavenumber range of 4-12 cm^{-1}. The details of the light source are described in ref. 3.

In order to obtain the radiation at the lower intensity the electron injection current of the accelerator gun was decreased.

ABSORPTION SPECTROSCOPY FOR SiO_2 POWDER: The nominal diameter of the fine SiO_2 particles is 26 nm. The sample 5 mm thick was sandwiched with two quartz plates 3 mm thick. Figure 2 shows the wavenumber dependence of the transmittance of light obtained for the sample and for only the sample holder. The periodical oscillation observed on the spectrum can be attributed to the interference between lights transmitting through the sample and those reflected at the surfaces of the quartz plates. In the results it was found that the ratio of the light absorbed by the sample to the incident light increased with the wavenumber from about 0.2 to 0.3 in this wavenumber range. In the other experiments the light intensity effect on the transmittance was observed, where any change in the surface conditions of the particles by the light irradiation was suggested.

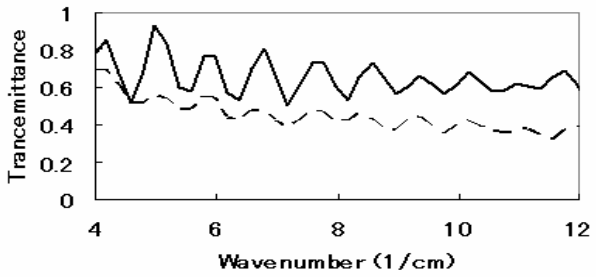

Fig. 2. Wavenumber dependence of light transmittance for the SiO_2 fine particles 5 mm thick sandwiched with two quartz plates 3 mm thick (dotted line): solid line shows the result for only the sample holder.

The results for the present work gave us the fundamental information about the powder sintering process using THz light as a source for heating and basic interaction between fine particles and THz light.

In order to investigate the intensity effect pump-probe experiments using the electron linac of Osaka Prefecture University are under preparation.

REFERENCES:

[1] T. Takahashi, T. Matsuyama, K. Kobayashi, Y. Fujita, Y. Shibata, K. Ishi and M. Ikezawa, Rev. Sci. Instrum. **69** (1998) 3770.
[2] S. Okuda, M. Nakamura, K. Yokoyama, R. Kato and T. Takahashi, Nucl. Instrum. Meth. **A445** (2000) 267.
[3] S. Okuda and T. Takahashi, Infrared Phys. Technol. **51** (2008) 410.
[4] S. Okuda, D. Komatsu, R. Taniguchi, T. Kojima and T. Takahashi, Proc. 5th Int. Symp. on Material Cycling Engineering（Mar. 10-11, 2010, Sakai, Japan) p. 111.

採択課題番号 21014　　ライナック電子線からのコヒーレントテラヘルツ放射による吸収分光　　共同通常

（阪府大・産学官）奥田修一、谷口良一、小嶋崇夫、小松大悟（京大・原子炉）高橋俊晴

CO4-5 Property of Linearly Polarized Coherent Transition Radiation Emitted from Wire-Grid Radiator

T. Takahashi

Research Reactor Institute, Kyoto University

INTRODUCTION: For the spectroscopic purpose, various types of coherent radiation emitted from a relativistic electron beam have attracted a considerable attention as a new and powerful light source in the THz-wave region. Coherent transition radiation (CTR) is one of such a light source. Whereas synchrotron radiation has linear polarization along an electron orbit, the electric vector of transition radiation (TR) emitted from a metallic screen is axially symmetric with respect to the trajectory of an electron beam. Therefore, CTR is usually utilized as a non-polarized light source in the spectroscopic application. However, circularly polarized light has been useful in the circular dichroism spectroscopy. Shibata *et al*. has developed a technique of generation of circularly polarized THz-wave radiation with the phase difference between the forward TR and the backward TR [1]. However, it was difficult to control the polarization degree because the geometrical arrangement was important in order to generate both the linearly polarized the forward and the backward TR. In this report the property of the linearly polarized CTR with a radiator of a wire grid has been experimentally investigated in order to develop a new technique of generation of circular polarized THz radiation.

EXPERIMENTAL PROCEDURES: The experiment was performed at the coherent radiation beamline [2] at the 40-MeV L-band linac of the Research Reactor Institute, Kyoto University. The width of the macro pulse and the repetition rate of the electron beam were 47 ns and 46 Hz, respectively. The average current of the electron beam was 1.8 μA. As the radiator of forward and backward CTR, wire-grid polarizers 10 μm thick with 25 μm spacing were used, respectively. The direction of grid of both polarizers was vertical. The spectrum of CTR was measured by the Martin-Puplett type interferometer.

RESULTS: The observed spectra, which were measured as varying the distance between the forward and backward radiators, are shown in Fig.1. The distance is usually called the emission length. The observed intensity uniformly decreases as shortening the emission length. In order to investigate the relation between the intensity and the emission length, observed data in fig.1 were plotted as a function of the emission length at some wavelengths in fig.2 on a log scale. When the emission length is far shorter than the formation length, the intensity of CTR is proportional to the square of the emission length [3]. The formation length in the millimeter-wave region is longer than 15 m for the 40-MeV electron beam. Each plots in fig.2 was fitted by the equation of $y=x^a$ in order to confirm the quadratic dependence in fig.2. The results were a=2.6 for the shorter wavelengths and a=3.0 for the longer wavelengths. These are larger than the expected value of 2. The reason of this discrepancy is not clear at present.

REFERENCES:

[1] Y. Shibata *et al.*, Rev. Sci. Instrum. **72** (2001) 3221.

[2] T. Takahashi *et al.*, Rev. Sci. Instrum. **69** (1998) 3770.

[3] Y. Shibata *et al.*, Phys. Rev. E **49** (1994) 785.

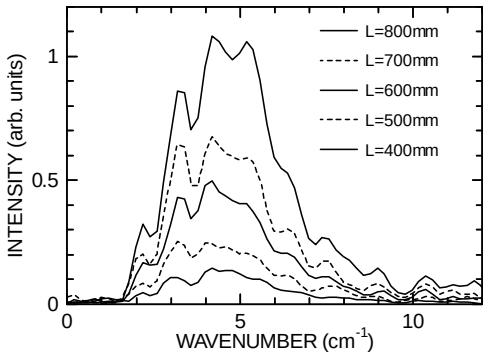

Fig.1. The observed spectra as varying the emission length.

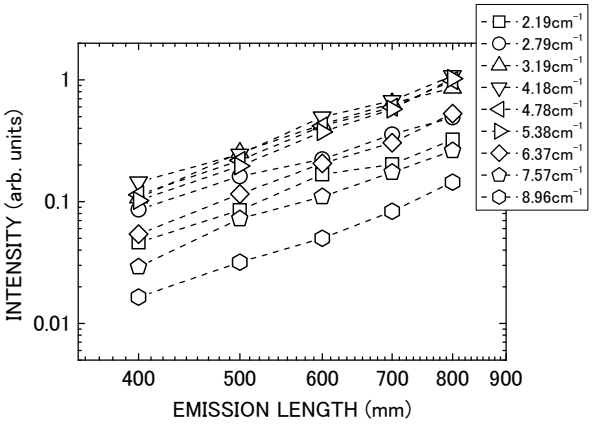

Fig.2. The relation between the observed intensity and the emission length at each wavenumber in fig.1.

採択課題番号 21015　極短パルスコヒーレント放射光を用いたテラヘルツ・ミリ波領域高時間分解分光法に関する研究　共同通常

（京大・原子炉）高橋俊晴、佐藤信浩、（東北学院大・工）淡野照義

CO4-6 Complete Decomposition of Pyrrolidone Derivatives by γ-Ray Irradiation under Heating

M. Nogami, T. Kawasaki, M. Harada and Y. Ikeda

Research Laboratory for Nuclear Reactors, Tokyo Institute of Technology

INTRODUCTION: We have been developing a novel reprocessing system for spent FBR fuels based on two precipitation processes[1]. In this system, only U(VI) species are firstly precipitated in nitric acid solutions dissolving spent fuels by using a pyrrolidone derivative (NRP) with low hydrophobicity and donicity which bring lower precipitation ability. Secondly the residual U(VI) and Pu(IV, VI) are precipitated simultaneously using another NRP with higher precipitation ability. Use of a slight excess amount of the precipitants is inevitable for complete precipitation of U and Pu species due to the solubility of the precipitates. Therefore, the residual precipitants included in the highly active waste solution (HAW) generated after the second precipitation treatment should be completely removed or decomposed for safer disposal of the wastes.

In our previous study, we have clarified that the stability of NRPs by γ-ray irradiation under heating is lower in HNO_3 of 6 mol·dm^{-3} (= M) than of 3 M[2]. Based on this knowledge, a positive decomposition of *N*-*n*-butyl-2-pyrrolidone (NBP) which is one of the NRPs with lower precipitation ability was examined by using HNO_3 of higher concentration under γ-ray irradiation and heating. The advantage of this method is that no special equipments are necessary for the treatment, because the increase in the concentration of HNO_3 of HAW is possible by feeding NOx gas or condensation.

EXPERIMENTS: A sample solution containing 0.1 M NBP and 9 M HNO_3 was used. γ-Ray irradiation was conducted under heating at 75 °C using the similar apparatus as previously reported[2]. The dose rate and the reaction time were 9.2 kGy·h^{-1} and 5h, respectively, meaning the total dose was 46 kGy. The irradiated sample solution was analyzed by ^{1}H and ^{13}C NMR (JEOL 400MHz, solvent: dimethyl sulfoxide-d_6).

RESULTS: ^{1}H NMR spectra of the sample solution before and after irradiation are shown in Fig. 1. It can be seen that the two signals assigned to (d) and (e) of NBP in the spectrum before irradiation completely disappear in the irradiated sample. This means that NBP does not exist in the irradiated sample. Figure 1 also shows a possibility of the existence of acetic acid (ca. 2.1 ppm, CH_3, singlet) and propionic acid (ca. 1.1 ppm, CH_3, triplet) in the irradiated sample. The signals between 2.3 and 2.4 ppm seem to consist of two components, and one of them is likely to be attributed to another signal of propionic acid (CH_2). In the ^{13}C NMR spectrum of the irradiated sample, the signal which should be attributed to the carbon atom of oxalic acid was detected at ca. 161 ppm. The above results support our proposal for the degradation mechanism of NBP in HNO_3 by γ-ray irradiation[3].

These facts indicate that NBP was completely decomposed to smaller organic compounds under the present irradiation condition. Further optimization of the condition for decomposing organic acids such as acetic acid and oxalic acid is necessary for the practical use. The use of higher temperature or longer reaction time is expected to be effective.

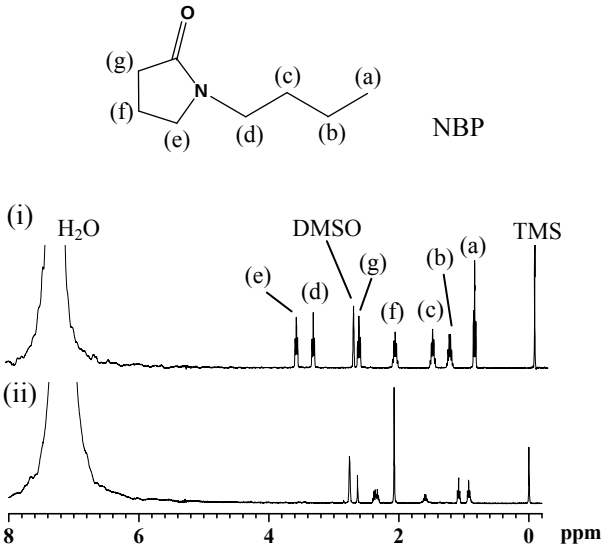

Fig. 1. Chemical structure of NBP and ^{1}H NMR spectra of NBP solution before and after irradiation; (i) before irradiation, (ii) after irradiation.

ACKNOWLEDGMENT: Present study is the result of "Development of Advanced Reprocessing System Using High Selective and Controllable Precipitants" entrusted to Tokyo Institute of Technology by the Ministry of Education, Culture, Sports, Science and Technology of Japan (MEXT).

REFERENCES:

[1] Y. Morita *et al.*, J. Nucl. Sci. Technol.**46** (2009) 1129-1136.
[2] M. Nogami *et al.*, KURRI Prog. Rep. **2008**, (2009) 185.
[3] M. Nogami *et al.*, JAEA-Review 2009-041 (2008) 25.

採択課題号 21020　アクチニルイオン配位性アミド化合物の耐ガンマ線性に関する研究　一般通常
（東工大・原子炉）野上雅伸、川崎武志、原田雅幸、池田泰久

CO4-7 Radiation-Induced Luminescence for Applying to Retrospective Dosimetry

H. Fujita, Y. Nakano[1] and T. Saito[1]

Nuclear Fuel Cycle Engineering Laboratories, JAEA
[1]Research Reactor Institute, Kyoto University

INTRODUCTION: It is well known that natural quartz exposed to prior ionizing radiation emits luminescence by subsequent exposure to heat or light, i.e., thermoluminescence (TL) or optically stimulated luminescence (OSL), respectively (e.g. [1, 2]). These luminescence signals have been widely applied to dating and retrospective dosimetry [3, 4]. Luminescence characteristics of natural quartz are dependent on their origins, thermal histories, impurity contents, etc [5]. However, emission mechanism of luminescence from Japanese quartz has not been explained, so far.
In this research, the emission mechanism of the luminescence was investigated in conjunction with various radiation induced phenomena after annealing treatments of quartz samples, involving TL, OSL and electron spin resonance (ESR) measurements. In this report, only the results of ESR measurements were described.

EXPERIMENTS: Soil samples were collected from three different locations around Tokai-mura, Ibaraki Prefecture in Japan. The samples were taken from depth of 0-50 mm at each location.
In our laboratory, these samples were treated with 6M sodium hydroxide (NaOH) and 6M hydrochloric acid (HCl) and then etched with 46% hydrofluoric acid (HF) to remove external α-irradiated outer layers of each grain [6]. Further purification of the quartz grains was performed by hand selection under a microscopic observation.
Prior to irradiation, a portion of the quartz was annealed for 24 h at 600 and 1000 ºC and the rest was annealed for 2 h at 500 ºC to eliminate natural luminescence components.
The quartz samples were irradiated with ^{60}Co source (1.5 kGy) at room temperature at the Kyoto University Research Reactor Institute (KURRI).
The quartz was irradiated with γ-ray at room temperature and was then stored for one day at the temperature to wait for decay of afterglow. After that, the ESR measurements were conducted using an ESR spectrometer (Jeol Ltd. JES-TE 200) at room temperature or -196 ºC, respectively. A part of the quartz was used in the ESR measurements after blue-LED illumination.

RESULTS: Figure 1 represents the typical ESR spectra from the quartz grains. Al-center signals and Ti-center signals were observed in Fig. 1 (a), unidentified center signals were also observed in Fig. 1 (b). These signals were reported by Fujita et al. [7] using other kinds of quartz grains. All of the samples used in the experiment showed Al-, Ti- and unidentified center signals in ESR measurements.
The behavior of the Al-, Ti- and unidentified center signals with annealed temperatures was similar to the results measured by Fujita et al. [7].
The comparison of ESR signals with blue-LED illumination and without one was carried out for all of quartz samples. The unidentified signals were decreased by the illumination. The signals could be related with luminescence source.
OSL and TL have not been measured using quartz samples irradiated by the ^{60}Co source yet because luminescence measurement system has been broken down. Therefore, the remained measurements will be carried out in 2010.

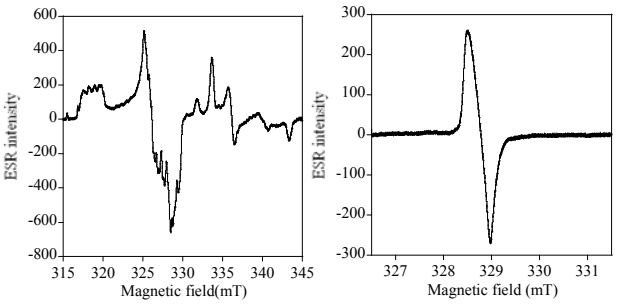

Fig. 1. ESR spectra in quartz grains. The spectra were measured at -196 **ºC** (a) and at room temperature (b) from quartz grains annealed at 1000 ºC for 24 h.

REFERENCES:

[1] T. Hashimoto *et al*., Radioisotopes **51** (2002) 10-18.
[2] T. Hashimoto *et al*., Radiat. Meas. **41** (2006) 1015-1019.
[3] H. Fujita *et al*., Radiat, Prot. Dosim. **123** (2007) 143-147.
[4] A. S. Murray *et al*., Radiat. Meas. **43** (2008) 776-780.
[5] T. Hashimoto *et al*., Radiat. Meas. **37** (2003) 479-485.
[6] M. J. Aitken, Oxford University Press (1998).
[7] H. Fujita *et al*., Radiat. Meas. **42** (2007) 156-162.

採択課題番号 21022　緊急時被ばく線量測定を目指した放射線誘起ルミネッセンスの基礎的研究　共同通常
（原子力機構、核サ研）藤田博喜、（京大・原子炉）中野幸廣、斉藤毅

CO4-8 Development of a Reflection-Mode Scanning Near-Field THz-Wave Microscopy with Coherent Transition Radiation

T. Takahashi, T. Iizuka [1] and S. Kimura [1, 2]

Research Reactor Institute, Kyoto University
[1]School of Physical Sciences, The Graduate University for Advanced Studies
[2]UVSOR Facility, Institute for Molecular Science

INTRODUCTION: The technique of near-field THz-wave microscopy is a characteristic application of coherent radiation emitted from a relativistic electron beam. This technique provides high spatial resolution below the diffraction limit. In the previous report [1] we obtained the spatial resolution power of λ/4 in the transmission mode. Reflection measurement is also important for the THz-wave spectroscopy. In the present report we has been experimentally investigated the property of near-field in the reflection mode using an aperture probe with coherent transition radiation (CTR).

EXPERIMENTAL PROCEDURES: The experiment was performed at the coherent radiation beamline [2] at the 40-MeV L-band linac of the Research Reactor Institute, Kyoto University. The width of the macro pulse and the repetition rate of the electron beam were 47 ns and 46 Hz, respectively. The charge of a bunch was 1.2 nC. The THz-wave source was CTR emitted from an aluminum foil with a thickness of 15-μm. The spectrum of CTR was measured by a Martin-Puplett type interferometer. The conical cone with an aperture of 775 μm in diameter was used as an illumination probe. Two types of optical setup were prepared in order to detect the reflected radiation. One was the beam-splitter type as shown in Fig.1 where the reflected radiation was divided by the Mylar beam splitter and guided to the Si bolometer. The other was the light-guide type as shown in Fig.2 where the reflected radiation by the sample was guided to the Si bolometer through the light guide with an inside diameter of 10 mm.

RESULTS: In order to investigate the spatial resolution, the edge of a stainless steel plate 0.3 mm thick was scanned as a sample in front of the aperture on the top of the illumination probe. The observed intensity of the reflected radiation is plotted in Fig. 3 and its first derivative is shown in Fig. 4. As the width of the derivative curve is equivalent to the spatial resolution, the resolution of 396 μm was derived from the Gaussian fitting of the derivative curve. In Figure 5, the observed CTR spectrum with a sample is shown by the dashed curve. The observed intensity remained without the sample as shown by the dotted curve, which was considered to be the stray light reflected by the inside of the probe. The calculated net spectrum reflected by the sample is represented by the solid curve. Considering the wavenumber of 5.7 cm^{-1} at peak intensity of this spectrum, the spatial resolution power was evaluated to be λ/4.4. Similarly, the resolution power of λ/4.6 was obtained in the light-guide type setup, which is equivalent value to that of the beam-splitter type.

ACKNOWLEDGMENTS: This work was partly supported by Quantum Beam Technology Program of MEXT, Japan.

REFERENCES:

[1] T. Takahashi, *et al.*, KURRI-PR 2008 (2009) CO4-10.

[2] T. Takahashi, *et al.*, Rev. Sci. Instrum. **69** (1998) 3770.

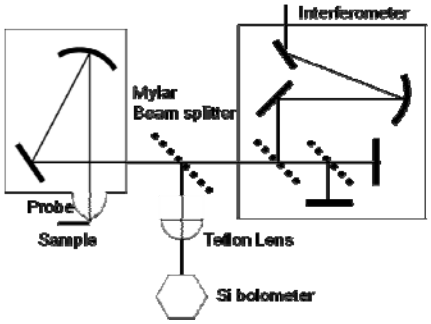

Fig. 1. Schematic layout of the optics of the beam-splitter type.

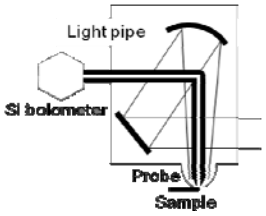

Fig. 2. Schematic layout of the optical setup of the light guide type.

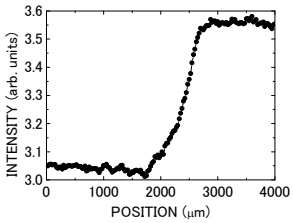

Fig. 3. Scanning curve of an edge of a SUS plate 0.3 mm thick.

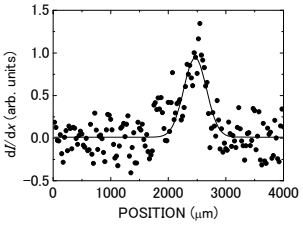

Fig. 4. First derivative curve of Fig. 3 and the Gaussian fitting (solid line).

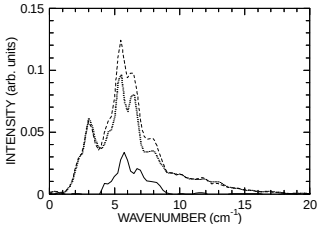

Fig. 5. Observed spectra of CTR with (dashed) and without (dotted) a sample. The solid curve shows the difference between the two spectra.

採択課題番号 21023　　コヒーレント遷移放射を用いたミリ波近接場イメージング　　共同通常分光法に関する研究

（分子研）木村真一、飯塚拓也、（京大・原子炉）高橋俊晴

CO4-9 Complex Structure of Ions Coordinated with Hydrophilic Polymer. 10:

A. Kawaguchi , Y. Gotoh[1] and Y. Morimoto

Research Reactor Institute, Kyoto University
[1]*Facuty of Text. Sci. and Tech., Shinshu Univ.*

INTRODUCTION: We have reported *in situ* composite structure through "secondary doping" by diffusion of metallic ions into the iodinated hydrophilic polymers. Polyiodide ions, I_n^- (n = 3, 5,,), which have been doped into the polymers previously, enhances following diffusion of other molecules or ions even through solution process at room temperature [1]. Then, if some precipitation process of inorganic salt advances there, produced salt grains can be regarded as fillers grown up from ions and stabilized in the polymers [2,3]. Consequently, such procedure provides hybrid (nano) composite without softening matrix, nor synthesis, nor melting, nor casting, nor blending [4].
In the case of silver ion (Ag^+) as following dopants, precipitation of AgI was predicted as nano-fillers which grew up from ionic diffusion and precipitation. However, we confirmed not only production of the inorganic salt, AgI, but other stages of the hybrid composite peculiar to process at inner volume of the polymers; at least, three stages (named as “stage I / II / III”) exist as composite structure and there is suggested a characteristic common to comprehensive matrix derived from many hydrophilic polymers [5-7]. These results suggest that process in the inner volume of the hydrophilic polymers presents both similarity and disparity to process in aqueous solution. Production of metallic salt at inner volume shows singular behaviors against ordinary precipitate given in solution; for example, existence of metallic salts precipitated in the matrix does not always ensure their same property as bulk in macroscopic scale.

EXPERIMENTS: As a starting PA6 (polyamide-6, Nylon^{TM}-6), commercial products of film ("Rayfan #1401" in thickness of 0.1mm, presented by Toray Film co.ltd.) were used. The cut pieces of filmy sample were immersed within an I_2-KI aqueous solution (0.2-0.8N) to prepare "PA6/polyiodide complex"; this procedure is called as "(first) iodine doping" [8,9]. To minimize effects by volatilizing elements, the "iodinated PA6" was aged in vacuum for more than two weeks. After drying in vacuum, the iodinated PA6 was immersed in a $AgNO_3$ aqueous solution of 0.2-1.0M("secondary doping"). Each doping process was terminated by rinsing the samples with distilled water.
Prepared samples ("stage II") were radiated with Ar-laser beam (λ = 514.5 nm, 200mW) in a quartz capillary at R.T. Or another sample was aged in a humid desiccator under applying DC static voltage field(1.2-1.5x10^3 V/m, in RH ~ 97%).

RESULTS AND DISCUSSION: In general environment of process in aqueous solution, association between metallic ion, Ag^+, and iodide ion, I^-, certainly induces precipitation of silver iodide, AgI, which indicates light-yellow color, and its grain grows up without spatial restriction($Ag^+ + I^- \rightharpoonup AgI\downarrow$). And, since one of stages, "stage II", also shows the same color and the same WAXD pattern as the AgI precipitate, grains of the filler are concluded as AgI [5].
However, the AgI filler grains precipitated in polymer also show peculiarity against ordinary bulk salt. For example, bulk AgI which was produced from solution or melt behaves as metallic salt with very low solubility in water, or its sensitivity for visible light is not so high[10,11]. On the other hand, "stage II" in the composite which contains AgI grains as nano-filler precipitated within inner volume of the hydrophilic polymers showed different behavior; it changed its color from light-yellow to gray by visible laser beam, or it responded for static DC field (Fig.1). Or, we reported decrease in size of the filler grains under humid environment through observation with SANS method [12]. These results suggest specific similarity and singularity of the AgI grains against its bulk salt; the former precipitated at inner volume of polymer does not always behave as the latter even though the filler grains in both give the same lattice constants for its crystal structure. It is assumed that restricted environment of inner volume of polymer distinctly affects growth of the salt grains.

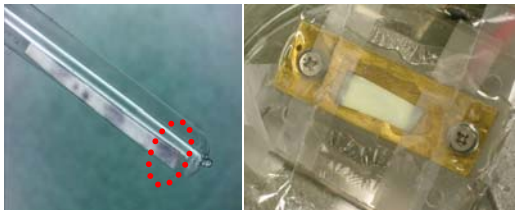

Fig. 1. Laser beam radiation (left) or DC-field applying (right) induced color change of "stage II" sample.

REFERENCES:

[1] A. Kawaguchi, *Sens. Actuators B*, **73** (2001) 174-178.
[2] A. Kawaguchi, *et.al*., *Polym. Prep. Jpn.*, **51** (2002) 393-393.
[3] Y. Gotoh, *et.al*., *ibid*., **51** (2002), 2259-2259.
[4] submitted as patent. (2006)
[5] A. Kawaguchi, *et.al*., *Polym. Prep. Jpn.*, **52** (2003) 577-577.
[6] A. Kawaguchi, *et.al*., *ibid.*, **55** (2006) 1004-1004.
[7] A. Kawaguchi, *et.al*., *ibid.*, **57** (2008) 3137-3137.
[8] A. Kawaguchi, *Polymer*, **33** (1992) 3981-3984.
[9] A. Kawaguchi, *et.al*., *Macromolecular Symposia*, **202** (2003) 77-83.
[10] *"Jikken Kagaku Guidebook"*, (ed. The Chem. Soc. Jpn., in Japanese) (1984).
[11] von E. Klein, *Photographische Korrespondenz* (in Germany), **92** (1956) 139-148.
[12] A. Kawaguchi, *et.al*., *KURRI Prog. Rep. 2002*, (2003) 20-20.

CO4-10 Monolayer Formation of Poly(methyl-*n*-propylsilane) on PEG Aqueous Solution

N. Sato, M. Tanimura and T. Matsuyama

Research Reactor Institute, Kyoto University

INTRODUCTION: In our previous studies, we have established the methodology for fabricating nanofilms made from hydrophobic polysilanes through γ-ray-induced grafting of hydrophilic monomers onto hydrophilic polymers and subsequent preparation of Langmuir films. In general, polysilanes are synthesized by the severe reaction using sodium metal, which fact causes difficulty for obtaining amphiphilic polysilanes with reactive functional groups in the side chain. We found, however, that γ-ray-induced grafting of hydrophilic monomers (e.g., methyl methacrylate) onto hydrophobic polysilanes (e.g., poly (methyl-*n*-propylsilane) (PMPrS)) yields amphiphilic polysilanes that can form monolayer on the water surface.

In the process of examining spreading property of amphiphilic polysilanes and hydrophobic polysilanes on the water surface, an interesting phenomenon was found. Surface pressure – Area isotherms showed that hydrophobic PMPrS spreads over the water surface in the presence of poly(ethylene glycol) (PEG) in the subphase water. Those spread PMPrS monolayers can be transferred onto solid substrates, as is proved by characteristic UV absorption spectra of polysilanes from the substrates. Close investigation into this phenomenon can lead to the new technique for preparing nanofilms without any chemical modification of polysilanes.

Although the transfer of PMPrS onto the solid substrate is confirmed, it is still unknown whether PEG in the subphase water is also transferred onto the solid substrates. In this study, we examined the presence of PEG molecules on the transferred film by measuring UV spectra of pyrene groups introduced in the PEG main chain as a chromophore.

EXPERIMENTS: PMPrS was synthesized by the conventional Wurtz-type coupling reaction of methyl-*n*-propyldichlorosilane. The molecular weight was 18000. PEG (molecular weight 6000) was used for the following synthesis as purchased. Pyrene-labeled PEG (PEG-Py) was synthesized by the reaction of PEG and 1-pyrenebutylic chloride. An aqueous solution of PEG-Py (concentration: 2.0×10^{-3} monomer unit mol/L) was used as the subphase water, onto which a toluene solution of PMPrS was dropped. The formed monolayer was transferred onto a hydrophilic quartz substrate by the vertical dipping method. After that, the transferred monolayer was rinsed with dichloromethane, and the rinsed solution was used for the UV absorption spectrum measurement.

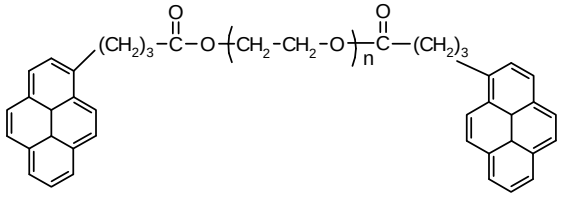

Fig. 1. Structure of pyrene-labeled PEG

RESULTS AND DISCUSSION: A dichloromethane solution of synthesized PEG-Py shows the same UV spectrum as the low-molecular model compounds, 1-pyrenebutyric acid (PBA), indicating that the pyrene was successfully attached to the ends of PEG chains. As a result of calculation from absorbance of the solution and the molar extinction coefficient of the pyrene molecule, the labeling ratio of pyrene was evaluated as 182%. Since one PEG chain has two ends, this means that almost all the ends were labeled by pyrene.

Surface pressure – Area isotherms of PMPrS on the PEG-Py aqueous solution shows a more expanded profile than that on a non-labeled PEG aqueous solution. The limiting occupied area is 0.22 nm^2/Si-unit, which is larger than the value for the non-labeled PEG subphase, 0.17 nm^2/Si-unit. This result suggests that hydrophobic pyrene groups floating on the surface of the subphase.

The monolayer formed on the subphase PEG-Py aqueous solution was transferred onto a quartz substrate in the transfer ratio of 1.1, proving that the monolayer was fully transferred.

A dichloromethane solution obtained by rinsing and dissolving the transferred monolayer shows UV spectrum as shown in Fig. 2. The difference spectrum from PMPrS solution almost conforms to the PBA solution spectrum, indicating that PEG-Py is transferred onto the solid substrate together with PMPrS. The molecular number ratio of PMPrS to PEG-Py, which is evaluated from the absorbance ratio, is found to be 1:1.98.

From above results, it can be said that a kind of interfacial complex of PMPrS and PEG acts like amphiphilic molecules to form monolayers which is transferable onto solid substrates.

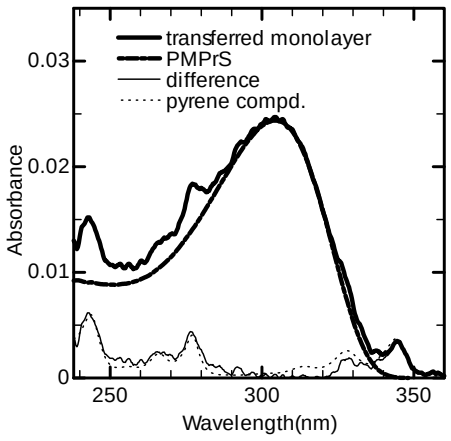

Fig. 2. UV spectra of the re-dissolved transferred monolayer in comparison with those of PMPrS and PBA.

採択課題番号 21043　機能材料創製におけるクリーンプロセスとしての放射線利用　共同通常
（京大・原子炉）佐藤信浩、（山形大工）皆川雅朋、（京大原子炉）徐虬